Open access dataset of holographic videos for codec analysis and machine learning applications

Antonin Gilles, Patrick Gioia, Nabil Madali, Anas El Rhammad, Luce Morin

Open access dataset of holographic videos for codec analysis and machine learning applications

Antonin Gilles[1*] Patrick Gioia[1,2] Nabil Madali[1] Anas El Rhammad[1] Luce Morin[1,3]

[1] IRT b<>com Cesson-Sévigné France
[2] Orange Labs Cesson-Sévigné France
[3] INSA Rennes Rennes France

Abstract

Despite the growing interest for Holography, there is a lack of publicly available three-dimensional hologram sequences for the evaluation of video codecs with inter-frame compression mechanisms such as motion estimation and compensation. In this paper, we report the first large-scale dataset containing 18 holographic videos computed with three different resolutions and pixel pitches. By providing the color and depth images corresponding to each hologram frame, our dataset can be used in additional applications such as the validation of 3D scene geometry retrieval or deep learning-based hologram synthesis methods. Altogether, our dataset comprises 5400 pairs of RGB-D images and holograms, totaling more than 550 GB of data.

Keywords : Real-time Hologram Calculation, Computer-Generated Holography, 3D Imaging

1 Introduction

With the recent advances in capture and display systems, holography attracted a significant interest from the scientific and industrial communities during the last decade. Indeed, since it provides all the depth perception cues of the human visual system without causing eye-strain, it is often considered as a perfect candidate for the ultimate 3D display creating virtual images indistinguishable from the real ones [1].

However, one of the most important obstacles to the adoption of Holography for 3D visualization applications is the massive amount of information contained in digital holograms [2]. As a consequence, and since they have very different signal properties compared to conventional images and videos, specific compression techniques need to be designed for holographic data [3–7]. In this context, the Joint Photographic Experts Group (JPEG) designed a new standard for the compression of holograms, called JPEG Pleno Holography [8,9]. To define the common test conditions necessary for the objective and subjective quality evaluation of proponents codecs [10], the JPEG committee gathered test data from publicly available hologram databases [11–14].

While they cover a wide range of use cases, resolutions and pixel pitches, the aforementioned databases are mainly restricted to still holographic images. Providing an open access dataset of dynamic hologram sequences is therefore essential for the evaluation and comparison of video coding algorithms with inter-frame compression mechanisms such as motion estimation and compensation. In this paper, we propose the first large-scale holographic video dataset containing 18 sequences of 300 hologram frames, computed with three different resolutions and pixel pitches. For each hologram, the corresponding color and depth images are also provided, enabling their use in additional applications such as the validation of 3D scene geometry retrieval or deep learning-based hologram synthesis methods. Altogether, our dataset comprises 5400 pairs of RGB-D images and holograms, totaling more than 550 GB of publicly available data[1].

The remainder of this paper is organized as follows. Section 2 presents the synthetic scenes, calculation parameters and method used to compute the holographic videos, Section 3 describes the proposed dataset structure and usage, and Section 4 outlines its potential ap-

*This work has been achieved within the Research and Technology Institute b<>com, dedicated to digital technologies. It has been funded by the French government through the National Research Agency (ANR) Investment referenced ANR-A0-AIRT-07. Corresponding author can be reached at {antonin.gilles@b-com.com.

[1] https://hologram-repository.labs.b-com.com/#/holographic-videos

plications, including the design and assessment of video codecs and the validation of 3D scene geometry retrieval or deep learning-based hologram synthesis methods. Finally, Section 5 discusses the current limitations and future extensions of the proposed dataset.

2 Holographic video acquisition

In the following, we describe the 3D scenes, calculation parameters, and Computer-Generated Hologram (CGH) method used to compute the proposed holographic dataset.

2.1 Input synthetic 3D scenes

Figure 1 shows the six synthetic scenes used to compute the holographic videos, which contain the following 3D models:

- *Animals* – a fox, a rabbit and a bear
- *Cars* – two cars, a garbage truck and a bus
- *Dices* – three dices in front of a chessboard
- *Piano* – a piano and its chair
- *Table* – a table surrounded by four chairs
- *Woods* – a mushroom house with four trees

From one frame to another, the hologram position was shifted along a given path shown in green in Figure 1, with its optical axis always pointing towards the scene center. In addition, while *Cars*, *Dices*, *Piano*, *Table* and *Woods* are still 3D scenes, the models contained in *Animals* are animated.

2.2 Calculation parameters

Table 1 shows the hologram calculation parameters used to compute the holographic videos. For each scene, we computed three sequences of 300 hologram frames with different resolutions and pixel pitches, called configurations 1, 2 and 3. These configurations enable a wide range of testing conditions: while the maximum diffraction angle is lower than 2.87° for the first configuration, it is more than six times larger in the third one, reaching 13.7°, 15.4° and 18.7° for the red, green and blue channels, respectively.

To subjectively assess their visual quality, the proposed holographic videos can be either numerically reconstructed or optically displayed on Spatial Light Modulators (SLM). Indeed, even though configuration 3 does not correspond to any commercially available SLM at the time of writing, the holograms computed using configurations 1 and 2 are compatible with the Thorlabs EXULUS-HD1 and EXULUS-4K1 SLMs, and with the HoloEye LETO-3 and GAEA-2 SLMs, respectively. Nevertheless, to this end the sequences first need to be converted and quantized to real-valued amplitude or phase-only holograms, as detailed in Section 3.3.

2.3 Hologram synthesis method

To compute the holographic videos, we used a layer-based CGH calculation method with occlusion culling. For each hologram frame H of resolution $(N_x \times N_y)$ and pixel pitch p, the method comprises four steps, which are described in the following.

Let $\mathcal{R}_H$ be the local coordinates system of H, whose origin is located at the center of the hologram and whose axes $\mathbf{x}$, $\mathbf{y}$ and $\mathbf{z}$ correspond to its horizontal, vertical and optical axes, respectively. The first step of our method is to capture a 2D-plus-depth orthographic projection of the scene from the hologram position. To this end, we use a virtual camera of resolution $(N_x \times N_y)$ whose projection matrix is given by

$$P = \begin{bmatrix} N_y & 0 & 0 & N_x/2 \\ 0 & N_y & 0 & N_y/2 \\ 0 & 0 & 0 & 1 \end{bmatrix} T, \tag{1}$$

where T is the (4×4) transformation matrix from the world coordinates system to the hologram coordinates system $\mathcal{R}_H$.

Then, the 3D scene geometry is reconstructed from the acquired 2D-plus-depth data. Let A and D be the color and depth images captured by the camera. Since D is encoded as an 8-bits gray level image, the scene geometry is naturally sliced into 256 parallel depth layers located at depths

$$z_d = \frac{d}{255}(z_{\max} - z_{\min}) + z_{\min}, \tag{2}$$

and separated by a distance

$$\Delta = \frac{z_{\max} - z_{\min}}{255}, \tag{3}$$

where $d \in \{0, ..., 255\}$ is the layer index and $z_{\min}$, $z_{\max}$ are the minimal and maximal depths of the scene, respectively.

Each depth layer is thus considered to operate as a surface source of light emitting a complex wave o_d sampled on a regular grid of resolution (N_x, N_y), such that

$$o_d[x, y; c] = \begin{cases} A[x, y; c] \exp\left(j\phi[x, y]\right) & \text{if } D[x, y; c] = d \\ 0 & \text{otherwise,} \end{cases} \tag{4}$$

Table 1: Hologram calculation parameters

Parameter	Configuration 1	Configuration 2	Configuration 3
Frames	300	300	300
Width	1920	3840	2048
Height	1080	2160	2048
Pixel pitch	6.4 μm	3.74 μm	1 μm
Wavelength	Red: 640 nm Green: 532 nm Blue: 473 nm		
Maximum diffraction angle	Red: 2.87° Green: 2.38° Blue: 2.12°	Red: 4.91° Green: 4.08° Blue: 3.63°	Red: 18.7° Green: 15.4° Blue: 13.7°
Compatible SLMs	EXULUS-HD1, LETO-3	EXULUS-4K1, GAEA-2	-

where c is the color channel and $\phi[x, y] \in [0; 2\pi[$ is the initial phase, set to a uniform random value to render a diffuse scene. The light waves scattered by the scene are then numerically propagated and occluded from one layer to another using the recurrence formula

$$\begin{cases} u_{255} = o_{255} \\ u_d = o_d + m_d \mathcal{P}_\Delta \left\{ u_{d+1} \right\} \quad \text{for } 0 \leq d < 255. \end{cases} \tag{5}$$

In this last equation, u_d is the light wave propagated on layer d, m_d is a binary cross-section mask which has value 0 when $D[x, y; c] = d$ and 1 elsewhere, and $\mathcal{P}_z$ stands for the Angular Spectrum propagation [15] between two parallel planes separated by a distance z, given by

$$\mathcal{P}_z \left\{ u \right\} = \mathcal{F}^{-1} \left\{ \mathcal{F} \left\{ u \right\} (f_x, f_y) \, \mathrm{e}^{j 2\pi z \sqrt{\lambda^{-2} - f_x^2 - f_y^2}} \right\}, \tag{6}$$

where λ is the wavelength of light, f_x and f_y are the spatial frequencies, and $\mathcal{F}$ and $\mathcal{F}^{-1}$ are the forward and inverse Fourier Transform, respectively.

Finally, the light wave is numerically propagated towards the hologram plane to obtain the final hologram, such that

$$H = \mathcal{P}_{z_{\min}} \left\{ u_0 \right\}. \tag{7}$$

3 Dataset description and usage

In this section, we describe the dataset structure and how to numerically or optically reconstruct the holograms.

3.1 Dataset structure

Each holographic video is stored as a sequence of binary Matlab® v7.3 files containing the following variables:

projMatrix Transformation matrix from the world coordinates system to the hologram coordinates system T, of size (4×4)

amplitude Amplitude image A, stored as a table of $(N_y \times N_x \times 3)$ unsigned 8-bits integers

depthMap Depth map D, stored as a table of $(N_y \times N_x \times 3)$ unsigned 8-bits integers

depthMin Minimal depth of the scene $z_{\min}$, in meters

depthMax Maximal depth of the scene $z_{\max}$, in meters

hologram Computed hologram H, stored as a table of $(N_y \times N_x \times 3)$ single precision complex numbers

pixelPitch Pixel pitch p, in meters

wavelength Color wavelengths λ, in meters

3.2 Numerical reconstruction

To facilitate their visual quality assessment, each hologram can be reconstructed using the Numerical Reconstruction Software for Holography (NRSH) developed by the JPEG Pleno committee [16]. To this end, we provide for each hologram sequence the corresponding NRSH configuration file. For instance, the numerical reconstructions shown in the right column of Figure 2 were obtained using the following Matlab code:

```
% Initialize the reconstruction distance
% based on the depth map value d
zrec = d * (depthMax - depthMin) / 255 + depthMin;

% Initialize configuration file
info = getSettings('cfg_file', 'config.txt');

% Reconstruct hologram
recons = nrsh(hologram, zrec, info);
```

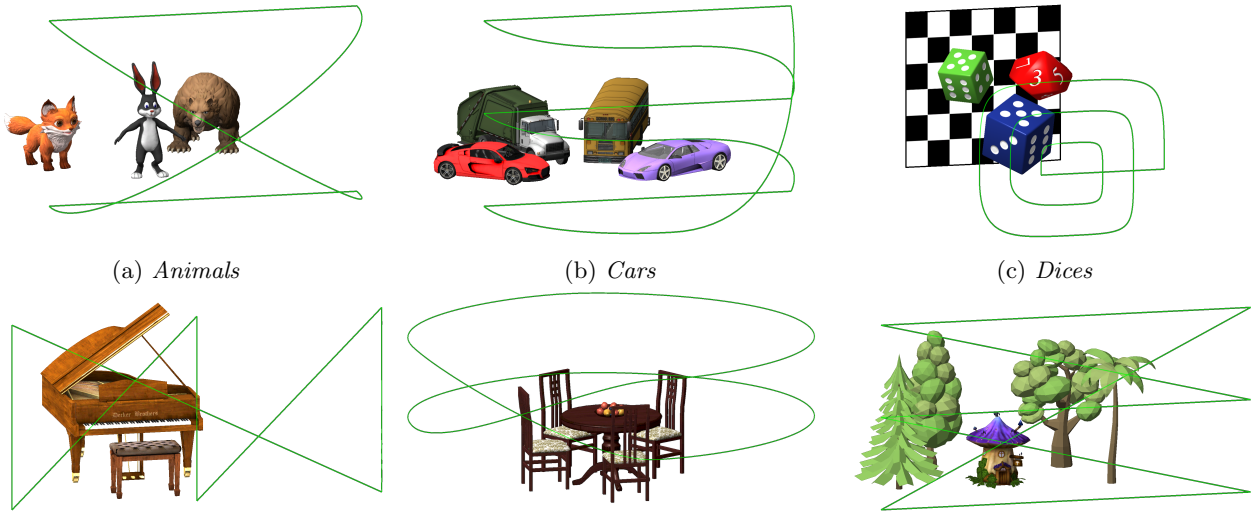

(a) *Animals* (b) *Cars* (c) *Dices*

(d) *Piano* (e) *Table* (f) *Woods*

Figure 1: Input 3D scenes used to compute the holographic dataset. For each scene, the hologram path is shown in green.

3.3 Optical reconstruction

As stated in Section 2.2, it is possible to optically display the hologram sequences on a SLM. To this end, the holograms first need to be converted and quantized to real-valued amplitude or phase holograms, which modulate the amplitude or phase of the reference wave, respectively.

The most straightforward way to compute an amplitude hologram is to numerically simulate the physical interference phenomena between the object and reference waves occurring in conventional optical holography, such that

$$\begin{aligned} H_{amplitude} &= (H+R)(H+R)^* \\ &= |H|^2 + |R|^2 + 2\Re\{HR^*\}, \end{aligned} \tag{8}$$

where $\Re\{C\}$ and C^* are respectively the real part and complex conjugate of C, and R is the incident reference wave in the hologram plane.

Since they do not modulate the amplitude of the incident wave, phase holograms have a better diffraction efficiency than amplitude holograms. However, the calculation of a phase hologram from the complex-valued scene light wave is a nonlinear ill-posed inverse problem for which analytic solutions cannot be found. Therefore, phase holograms are often computed using iterative phase retrieval algorithms such as the Gerchberg-Saxton method and its improved forms [17–19]. To avoid iterative methods, another approach is to use the double phase encoding algorithm [20, 21], which encodes each pixel of the complex-valued hologram using two phase values, or the complex error diffusion method [22, 23], in which the amplitude of each pixel is forced to unity and the resulting error is diffused to the adjacent values.

4 Applications

In the following, we present the applications of the proposed dataset, ranging from the design and assessment of holographic video codecs to the validation of 3D scene geometry retrieval or deep learning-based hologram synthesis methods.

4.1 Design and assessment of video codecs

First, this dataset may be used to facilitate the design of video coding algorithms with inter-frame compression mechanisms such as motion estimation and compensation. As a matter of fact, removing temporal redundancies would significantly reduce the memory and bandwidth consumption of holographic videos. It is thus envisioned that future coders will require this feature. However, since the light wave scattered by each scene point may contribute to every pixel during hologram recording, a slight change in the scene translates to substantially different hologram patterns. As a consequence, automated

motion estimation from holographic data is still a very challenging research topic [24].

Since *Cars*, *Dices*, *Piano*, *Table* and *Woods* contain only still 3D objects, the global scene motion from one frame to another can be perfectly induced from the transformation matrix T. By providing this matrix together with the 2D-plus-depth projections of the scene, the relation between the scene motion and resulting hologram can be easily characterized, constituting a valuable insight for the development of motion estimation and compensation algorithms. For instance, this data can be used to train a neural network for the prediction of scene object motion vectors from consecutive holographic video frames. It must be noted that since the hologram path is looped in each video sequence, the first and last holographic frames can be considered as being consecutive, enabling the use of any chunk of successive frames for the training, validation and test sets.

Once specific holographic video codecs have been developed, this dataset can be used to evaluate and compare their rate-distortion performances. While several objective or subjective quality evaluation procedures were specifically designed for still holograms of 3D scenes [25–27], new procedures need to be developed for holographic videos.

4.2 Deep learning-based hologram synthesis

The proposed holographic sequences may also find application in the field of supervised deep learning-based hologram synthesis methods. Indeed, over the last decade several techniques were proposed to generate holograms of 3D scenes using Deep Neural Networks (DNN), outperforming physically-based conventional CGH methods [28–30]. An extensive review of these works can be found in [31].

The supervised deep learning-based hologram calculation is formulated as follows. We call $\hat{H} = \mathcal{N}(\mathcal{X}, \Theta)$ the hologram predicted by the DNN function $\mathcal{N}$, where $\mathcal{X} = \{A, D\}$ is the input RGB-D image and Θ are the networks parameters. The network is trained by solving the minimization problem

$$\underset{\Theta}{\text{minimize}}\, \mathcal{L}\left\{\mathcal{N}(\mathcal{X}, \Theta), H\right\}, \tag{9}$$

where $\mathcal{L}$ is a loss function to evaluate the error between $\hat{H}$ and the ground-truth hologram H. In [32], the authors used this approach to design a Convolutional Neural Network (CNN) able to generate full-HD holograms at 60 Hz on a single consumer-grade graphics processing unit, at 1.1 Hz on a mobile device (iPhone 11 Pro) and at 2.0 Hz on an edge device with a Google Tensor Processing Unit (TPU).

Similarly to most deep learning-based methodologies, the main drawback of this approach is the large amount of data needed to train the DNN. In [32], the authors introduced the MIT-CGH-4K, an open-access dataset comprising 4000 pairs of RGB-D images and corresponding 3D holograms. Nevertheless, the MIT-CGH-4K holograms have a very limited space-bandwidth product: they were computed with a unique pixel pitch of 8 μm and a resolution of (384×384), which is insufficient for wide-viewing angle and large-scale visualisation. In addition, they were synthesized from different scenes and do not form a video sequence, preventing neural networks from learning inter-frame redundancy removal procedures to reduce the hologram calculation time.

The proposed dataset solves these limitations and can be used for the training, validation or test sets of DNN-based hologram synthesis methods. To increase the amount of data and reduce over-fitting during the training phase, the following data augmentation techniques can be used:

- rotating, shifting or flipping the RGB-D image along the vertical or horizontal axis results in the same transformations of the corresponding hologram;
- adding a constant offset value to the depth image can be compensated by propagating the hologram by the corresponding distance using the Angular Spectrum method given in Eq. (6).

4.3 Depth map or 3D scene geometry retrieval

Finally, the proposed dataset may also be useful in the field of depth map or 3D scene geometry retrieval from holographic data. As a matter of fact, retrieving the scene geometry from a single hologram would pave the way for many practical applications such as holographic data segmentation, classification and editing, as well as motion estimation and compensation.

Unfortunately, retrieving the scene from a single digital hologram is still a very challenging research topic. Indeed, since each hologram pixel gathers the contributions of every scene points, the 3D information is scrambled into the holographic signal and cannot be retrieved using conventional image processing algorithms. While several autofocus methods were proposed for retrieving a single depth value from holograms [33], these methods cannot compute a full depth map of the scene required for the above-mentioned applications.

In [34], the authors used a depth-from-focus (DFF) approach to retrieve the RGB-D image of the scene from a given hologram. They latter extended their work using a CNN model to evaluate the focus level of each pixel in the reconstruction volume in [35] and using the phase space representation of the hologram in [36]. A preliminary version of our proposed holographic dataset was used to validate the DFF methodology in [34], as well as for the training, validation and test sets of DNNs in [35, 36]. This confirms the suitability of this dataset for machine learning applications.

5 Discussion

Despite its various potential applications, our dataset still presents two limitations. First, since it only contains 18 computer-generated hologram sequences rendered from six different synthetic 3D scenes, its variety of content may not be sufficient for more complex machine learning-based tasks. Secondly, it does not include any optically acquired hologram, limiting its subsequent applications and use cases.

In our future work, we aim to address these limitations by enhancing the dataset with holograms generated from more natural and realistic synthetic 3D content, along with holograms derived from real-world scenes. Additionally, we intend to incorporate a wider variety of hologram types based on research and standardization needs.

6 Conclusion

In this paper, we reported the first large-scale open access holographic video dataset containing 18 sequences of 300 hologram frames, computed with three different resolutions and pixel pitches. Our dataset is primarily intended for the design and quality assessment of holographic video coding engines with inter-frame compression mechanisms such as motion estimation and compensation. However, by providing the color and depth images corresponding to each hologram frame, it can also be used in many other applications such as the validation of 3D scene geometry retrieval or deep learning-based hologram synthesis methods.

At the time of writing, our dataset comprises 5400 pairs of RGB-D images and holograms, totaling more than 550 GB of data. Nevertheless, in a future work we intend to expand it with holograms derived from synthetic 3D content that are more natural and realistic, along with holograms generated from actual real-life scenarios. Additionally, we plan to provide a wider range of hologram types, depending on the research and standardization requirements.

References

[1] Pierre-Alexandre Blanche. Holography, and the future of 3D display. *Light: Advanced Manufacturing*, 2(4):446–459, December 2021. Publisher: Light: Advanced Manufacturing.

[2] Peter Schelkens, Ayyoub Ahar, Antonin Gilles, Raees Kizhakkumkara Muhamad, Thomas J. Naughton, Cristian Perra, Antonio Pinheiro, Piotr Stepień, and Malgorzata Kujawińska. Compression strategies for digital holograms in biomedical and multimedia applications. *Light: Advanced Manufacturing*, 3:1–21, June 2022. Publisher: Light: Advanced Manufacturing.

[3] Anas El Rhammad, Patrick Gioia, Antonin Gilles, and Marco Cagnazzo. Scalable Coding Framework for a View-Dependent Streaming of Digital Holograms. In *2019 IEEE International Conference on Image Processing (ICIP)*, pages 146–150, September 2019. ISSN: 2381-8549.

[4] Anas El Rhammad, Patrick Gioia, Antonin Gilles, and Marco Cagnazzo. Progressive hologram transmission using a view-dependent scalable compression scheme. *Annals of Telecommunications*, 75(5):201–214, June 2020.

[5] Tobias Birnbaum, David Blinder, Raees K. Muhamad, Colas Schretter, Athanasia Symeonidou, and Peter Schelkens. Object-based digital hologram segmentation and motion compensation. *Optics Express*, 28(8):11861–11882, April 2020. Publisher: Optical Society of America.

[6] Raees Kizhakkumkara Muhamad, Tobias Birnbaum, David Blinder, Colas Schretter, and Peter Schelkens. Binary hologram compression using context based Bayesian tree models with adaptive spatial segmentation. *Optics Express*, 30(14):25597–25611, July 2022. Publisher: Optica Publishing Group.

[7] Raees K. Muhamad, Tobias Birnbaum, David Blinder, Colas Schretter, and Peter Schelkens. INTERFERE: A Unified Compression Framework for Digital Holography. In *Digital Holography and 3-D Imaging 2022 (2022), paper Th4A.2*, page Th4A.2. Optica Publishing Group, August 2022.

[8] Peter Schelkens, Touradj Ebrahimi, Antonin Gilles, Patrick Gioia, Kwan-Jung Oh, Fernando Pereira, Cristian Perra, and Antonio M. G. Pinheiro. JPEG Pleno: Providing representation interoperability for holographic applications and devices. *ETRI Journal*, 41(1):93–108, February 2019.

[9] Raees Kizhakkumkara Muhamad, Tobias Birnbaum, Antonin Gilles, Saeed Mahmoudpour, Kwan-Jung Oh, Manuela Pereira, Cristian Perra, Antonio Pinheiro, and Peter Schelkens. JPEG Pleno holography: scope and technology validation procedures. *Applied Optics*, 60(3):641–651, January 2021. Publisher: Optical Society of America.

[10] Antonio M. G. Pinheiro, Joao Prazeres, Antonin Gilles, Tobias Birnbaum, Raees Kizhakkumkara Muhamad, and Peter Schelkens. Definition of common test conditions for the new JPEG pleno holography standard. In *Optics, Photonics and Digital Technologies for Imaging Applications VII*, volume 12138, pages 157–171. SPIE, May 2022.

[11] D. Blinder, A. Ahar, A. Symeonidou, Y. Xing, T. Bruylants, C. Schreites, B. Pesquet-Popescu, F. Dufaux, A. Munteanu, and P. Schelkens. Open access database for experimental validations of holographic compression engines. In *2015 Seventh International Workshop on Quality of Multimedia Experience (QoMEX)*, pages 1–6, May 2015.

[12] Antonin Gilles, Patrick Gioia, Rémi Cozot, and Luce Morin. Hybrid approach for fast occlusion processing in computer-generated hologram calculation. *Applied Optics*, 55(20):5459–5470, July 2016.

[13] Antonin Gilles, Patrick Gioia, Rémi Cozot, and Luce Morin. Computer generated hologram from Multiview-plus-Depth data considering specular reflections. In *2016 IEEE International Conference on Multimedia Expo Workshops (ICMEW)*, pages 1–6, July 2016.

[14] Marco V. Bernardo, António M. G. Pinheiro, and Manuela Pereira. Benchmarking coding standards for digital holography represented on the object plane. In *Optics, Photonics, and Digital Technologies for Imaging Applications V*, volume 10679, page 106790K. International Society for Optics and Photonics, May 2018.

[15] Joseph W. Goodman. *Introduction to Fourier Optics*. Roberts and Company Publishers, Englewood, Colo, 3rd edition, 2005.

[16] Tobias Birnbaum, David Blinder, Raees K. Kizhakkumkara Muhamad, Antonin Gilles, Cristian Perra, Tomasz Kozacki, and Peter Schelkens. A standard way for computing numerical reconstructions of digital holograms. In *Optics, Photonics and Digital Technologies for Imaging Applications VII*, volume 12138, pages 172–184. SPIE, May 2022.

[17] RW Gerchberg and Owen Saxton. A practical algorithm for the determination of the phase from image and diffraction plane pictures. *Optik*, 35(2):237–246, November 1971.

[18] Chien-Yu Chen, Wu-Chun Li, Hsuan-Ting Chang, Chih-Hao Chuang, and Tsung-Jan Chang. 3-D modified Gerchberg–Saxton algorithm developed for panoramic computer-generated phase-only holographic display. *JOSA B*, 34(5):B42–B48, May 2017.

[19] Lizhi Chen, Hao Zhang, Zehao He, Xiaoyu Wang, Liangcai Cao, and Guofan Jin. Weighted Constraint Iterative Algorithm for Phase Hologram Generation. *Applied Sciences*, 10(10):3652, January 2020. Number: 10 Publisher: Multidisciplinary Digital Publishing Institute.

[20] C. K. Hsueh and A. A. Sawchuk. Computer-generated double-phase holograms. *Applied Optics*, 17(24):3874–3883, December 1978. Publisher: Optica Publishing Group.

[21] Andrew Maimone, Andreas Georgiou, and Joel S. Kollin. Holographic Near-eye Displays for Virtual and Augmented Reality. *ACM Trans. Graph.*, 36(4):85:1–85:16, July 2017.

[22] Reiner Eschbach. Comparison of error diffusion methods for computer-generated holograms. *Applied Optics*, 30(26):3702–3710, September 1991. Publisher: Optica Publishing Group.

[23] P. W. M. Tsang and T.-C. Poon. Novel method for converting digital Fresnel hologram to phase-only hologram based on bidirectional error diffusion. *Optics Express*, 21(20):23680–23686, October 2013. Publisher: Optica Publishing Group.

[24] David Blinder, Ayyoub Ahar, Stijn Bettens, Tobias Birnbaum, Athanasia Symeonidou, Heidi Ottevaere, Colas Schretter, and Peter Schelkens. Signal processing challenges for digital holographic video display systems. *Signal Processing: Image Communication*, 70:114–130, February 2019.

[25] Ayyoub Ahar, Ayyoub Ahar, Maksymilian Chlipala, Tobias Birnbaum, Tobias Birnbaum, Weronika Zaperty, Athanasia Symeonidou, Athanasia Symeonidou, Tomasz Kozacki, Malgorzata Kujawinska, Peter Schelkens, and Peter Schelkens. Suitability analysis of holographic vs light field and 2D displays for subjective quality assessment of Fourier holograms. *Optics Express*, 28(24):37069–37091, November 2020. Publisher: Optica Publishing Group.

[26] Ayyoub Ahar, Tobias Birnbaum, Maksymilian Chlipala, Weronika Zaperty, Saeed Mahmoudpour, Tomasz Kozacki, Malgorzata Kujawinska, and Peter Schelkens. Comprehensive performance analysis of objective quality metrics for digital holography. *Signal Processing: Image Communication*, 97:116361, September 2021.

[27] João Prazeres, Antonin Gilles, Raees Kizhakkumkara Muhammad, Tobias Birnbaum, Peter Schelkens, and Antonio M. G. Pinheiro. Quality evaluation of the JPEG Pleno Holography Call for Proposals response. In *2022 14th International Conference on Quality of Multimedia Experience (QoMEX)*, pages 1–6, September 2022. ISSN: 2472-7814.

[28] Ryoichi Horisaki, Yohei Nishizaki, Katsuhisa Kitaguchi, Mamoru Saito, and Jun Tanida. Three-dimensional deeply generated holography [Invited]. *Applied Optics*, 60(4):A323–A328, February 2021. Publisher: Optica Publishing Group.

[29] Ji-Won Kang, Byung-Seo Park, Jin-Kyum Kim, Dong-Wook Kim, and Young-Ho Seo. Deep-learning-based hologram generation using a generative model. *Applied Optics*, 60(24):7391–7399, August 2021. Publisher: Optica Publishing Group.

[30] Jiachen Wu, Kexuan Liu, Xiaomeng Sui, and Liangcai Cao. High-speed computer-generated holography using an autoencoder-based deep neural network. *Optics Letters*, 46(12):2908–2911, June 2021. Publisher: Optica Publishing Group.

[31] Tomoyoshi Shimobaba, David Blinder, Tobias Birnbaum, Ikuo Hoshi, Harutaka Shiomi, Peter Schelkens, and Tomoyoshi Ito. Deep-Learning Computational Holography: A Review. *Frontiers in Photonics*, 3, 2022.

[32] Liang Shi, Beichen Li, Changil Kim, Petr Kellnhofer, and Wojciech Matusik. Towards real-time photorealistic 3D holography with deep neural networks. *Nature*, 591(7849):234–239, March 2021. Bandiera_abtest: a Cg_type: Nature Research Journals Number: 7849 Primary_atype: Research Publisher: Nature Publishing Group Subject_term: Computational science;Computer science;Displays;Optical manipulation and tweezers Subject_term_id: computational-science;computer-science;displays;optical-manipulation-and-tweezers.

[33] Elsa S. R. Fonseca, Paulo T. Fiadeiro, Manuela Pereira, and António Pinheiro. Comparative analysis of autofocus functions in digital in-line phase-shifting holography. *Applied Optics*, 55(27):7663–7674, September 2016.

[34] Nabil Madali, Antonin Gilles, Patrick Gioia, and Luce Morin. Automatic depth map retrieval from digital holograms using a depth-from-focus approach. *Applied Optics*, 62(10):D77–D89, April 2023. Publisher: Optica Publishing Group.

[35] Nabil Madali, Antonin Gilles, Patrick Gioia, and Luce Morin. Automatic depth map retrieval from digital holograms using a deep learning approach. *Optics Express*, 31(3):4199–4215, January 2023. Publisher: Optica Publishing Group.

[36] Nabil Madali, Antonin Gilles, Patrick Gioia, and Luce Morin. PSDFH: A Phase-Space-Based Depth from Hologram Extraction Method. *Applied Sciences*, 13(4):2463, January 2023. Number: 4 Publisher: Multidisciplinary Digital Publishing Institute.

Figure 2: Amplitude, depth map, hologram phase and numerical reconstruction corresponding to the same frame of each scene.